Current Biology, Vol. 13, 2179–2184, December 16, 2003, ©2003 Elsevier Science Ltd. All rights reserved. DOI 10.1016/j.cub.2003.12.002

A Flagellar Polycystin-2 Homolog Required for Male Fertility in *Drosophila*

Terry J. Watnick,[1,2] Ying Jin,[2] Erika Matunis,[3] Maurice J. Kernan,[4] and Craig Montell[2,*]

[1]Department of Medicine
Division of Nephrology
[2]Department of Biological Chemistry
[3]Department of Cell Biology and Anatomy
The Johns Hopkins University School of Medicine
Baltimore, Maryland 21205
[4]Department of Neurobiology and Behavior
The State University of New York at Stony Brook
Stony Brook, New York 11794

Summary

A common inherited cause of renal failure, autosomal dominant polycystic kidney disease results from mutations in either of two genes, *PKD1* and *PKD2*, which encode polycystin-1 and polycystin-2, respectively [1]. Polycystin-2 has distant homology to TRP cation channels [2] and associates directly with polycystin-1 [3, 4]. The normal functions of polycystins are poorly understood, although recent studies indicate that they are concentrated in the primary cilia of a variety of cell types [5–8]. In this report we identified a polycystin-2 homolog in *Drosophila melanogaster*; this homolog localized to the distal tip of the sperm flagella. A targeted mutation in this gene, *almost there (amo)*, caused nearly complete male sterility. The *amo* males produced and transferred normal amounts of motile sperm to females, but mutant sperm failed to enter the female sperm storage organs, a prerequisite for fertilization. The finding that Amo functions in sperm flagella supports a common and evolutionarily conserved role for polycystin-2 proteins in both motile and nonmotile axonemal-containing structures.

Results and Discussion

To identify polycystin-2-related proteins in fruit flies, we queried the *Drosophila* database with human polycystin-2. Four related proteins emerged from this analysis (Figure 1A), each of which displayed a number of features typical of mammalian polycystin-2. These included six putative transmembrane domains (TMDs), a pore loop between TMD5 and TMD6, and a large first extracellular loop between TMD1 and TMD2 (Figure 1B). Among the polycystin-2 related proteins, CG6504 (Amo; almost there) was the most similar to human polycystin-2 [9] and its close relatives PKD2L1 [10] and PKD2L2 [11, 12]. We screened a *Drosophila* cDNA library and isolated a full-length *amo* cDNA, which encoded a protein of 924 residues. The greatest sequence identity between Amo and human polycystin-2, PKD2L1, and PKD2L2 occurred over the TMDs and the C-terminal portion of the first extracellular loop (Figure 1B).

*Correspondance: cmontell@jhmi.edu

In order to gain insight into the function of *amo*, we determined its expression pattern. RT-PCR analysis revealed that expression began during larval development and persisted into adulthood (Figure 2A, left panel). When adults were separated by sex, *amo* RNA was found exclusively in the adult male body (Figure 2A, right panel). We raised anti-Amo antibodies and confirmed that the protein was detected in males but not female flies (Figure 2B, left panel). Amo protein was also absent from male offspring of females harboring a maternal-effect mutation (*tudor*) that prevents formation of the germline [13] (Figure 2B, right panel). Males derived from *tudor* females lack sperm but retain testes and accessory glands that produce seminal fluid and accessory gland proteins (Acps). Taken together, these data suggest that Amo is expressed in the male germline.

Because there were no existing mutations in *amo* and because there were no P elements nearby, we chose to disrupt this gene by using homologous recombination [14, 15]. The 6 kb targeting construct contained stop codons near the N-terminus as well as before and after TMD6 (Figure 2C). After producing transgenic flies containing a randomly inserted copy of the knockout construct, we screened for homologous recombinants in the germline of approximately 300 females. We identified two targeting events as well as an insertion at a nonhomologous position. As previously reported [14], ends-in recombination frequently results in a tandem duplication at the targeted locus. One of the legitimate targeting events had such a tandem duplication. Although one copy retained both mutations on the 3′ side of the I-SceI site (Figure 2C), the second had lost the 5′ mutation and was therefore wild-type. We subsequently used intragenic recombination [16] to generate flies that retained either the mutant (*amo^1*) or wild-type copy, as confirmed by DNA sequencing (Figure S1, in the Supplemental Data available with this article online). We demonstrated by Western blot analysis that the Amo protein was present in the line retaining only wild-type *amo* but was not detected in *amo^1* flies (Figure 2B). Given that the antibodies were raised to a region of Amo N-terminal to the stop codons, it appeared that the C-terminal truncation caused instability of the protein or that the stop codons caused nonsense-mediated mRNA decay.

Male flies homozygous for the *amo^1* mutation were almost completely infertile. Most single-pair matings between wild-type males and females produced large numbers of progeny (Figures 2D and 2E). In contrast, matings between single *amo^1* males and wild-type females resulted in few or no offspring (Figures 2D and 2E). Matings between *amo^1* females and wild-type males resulted in normal numbers of progeny (data not shown). To confirm that the male fertility defect was due to the targeted mutation in the *amo* gene, we introduced a wild-type rescue construct into *amo^1* flies by germline transformation. The wild-type transgene restored expression of the Amo protein in the *amo^1* mutant background and completely rescued the fertility defect (Fig-

A

	hPKD2		PKD2L		C.e. PKD2	
ID	Identity	E-value	Identity	E-value		
CG6504	40% (396)	$2e^{-80}$	39% (403)	$2e^{-82}$	33% (405)	$5e^{-60}$
CG13762	25% (312)	$8e^{-16}$	27% (315)	$5e^{-19}$	23% (328)	$1e^{-07}$
CG16793	21% (517)	$7e^{-15}$	19% (492)	$5e^{-11}$	18% (507)	$3e^{-04}$
CG9472	24% (332)	$2e^{-14}$	23% (329)	$6e^{-09}$	17% (297)	3.6

B

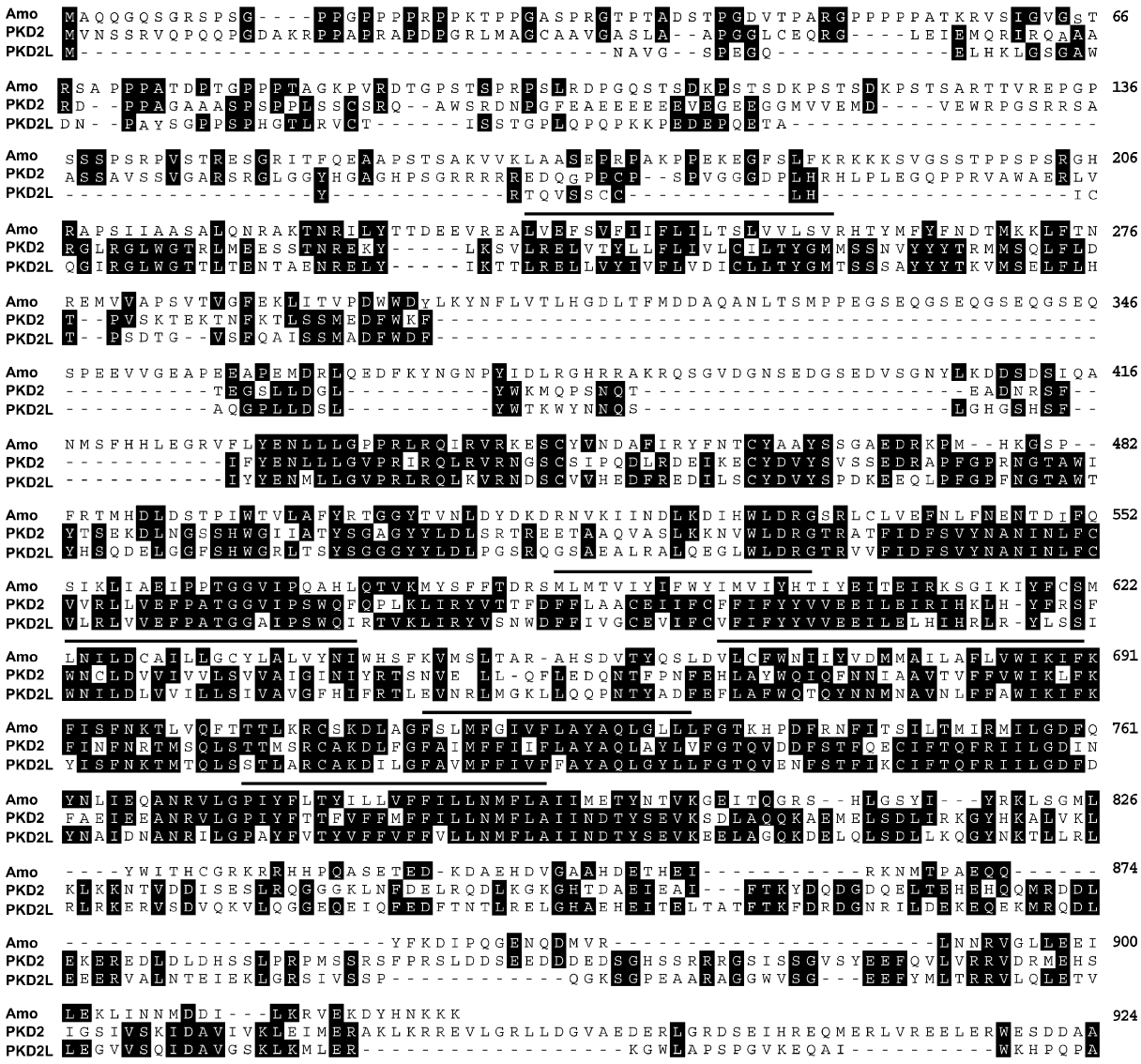

Figure 1. The *Drosophila* Polycystin-2-Related Gene, *amo*

(A) Amino acid sequence identities and E values obtained from the BLAST scores. The query sequences are indicated at the top: human polycystin-2 (hPDK2), human PKD2L1 (PKD2L), and *C. elegans* LOV-2 (*C. elegans* PKD2). The lengths of the amino acid identities are indicated in parentheses. The identification numbers of the *Drosophila* genes are indicated to the left.

(B) Amino acid alignment. Horizontal lines are placed above the six putative transmembrane segments. The residue numbers in the Amo amino acid sequence are indicated to the right. The C-terminal 46 and 43 residues of PKD2 and PKD2L, respectively, are not shown.

ures 2B, 2D, and 2E) as well as all other aspects of the phenotype described below.

We were able to exclude many etiologies that could account for the fertility defect observed in *amo*^{1} mutant flies. Testes from *amo*^{1} flies displayed normal architecture with a typical abundance of germ cells (data not shown). We assessed the motility of *amo*^{1} sperm by examining the rate of beating flagella and found it to be indistinguishable from that of the wild-type (see Supplemental Experimental Procedures). Furthermore, mutant males displayed normal courtship behavior and normal copulation latency and duration (data not shown).

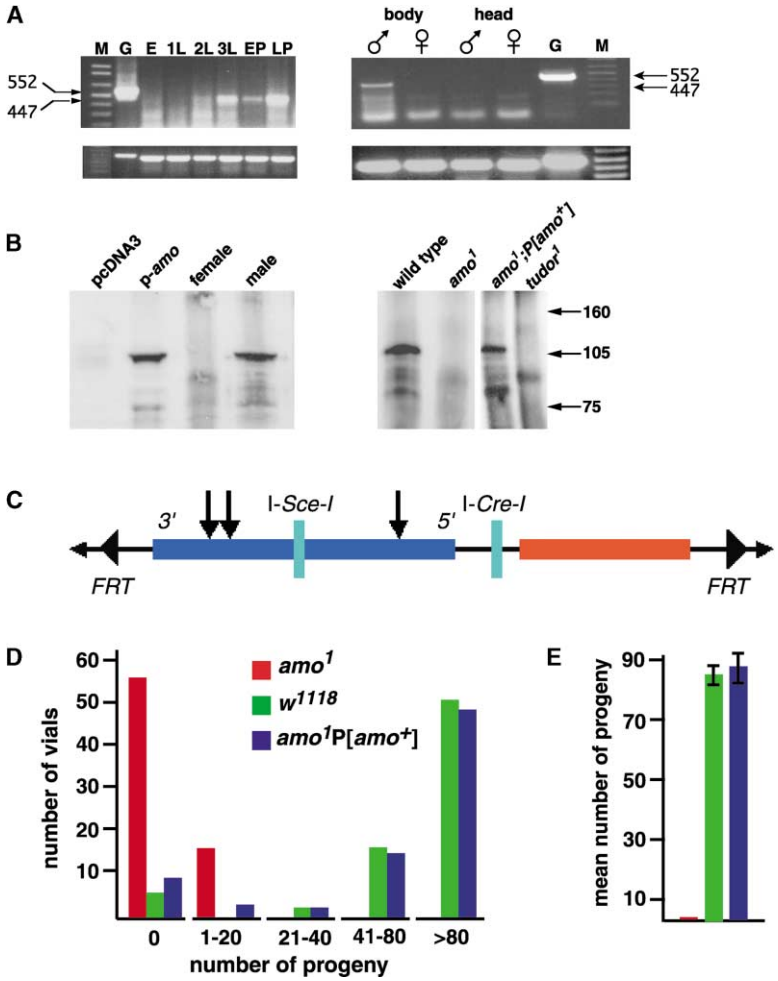

Figure 2. *amo* Is Expressed Exclusively in Males and Is Required for Male Fertility

(A) Expression of *amo* RNA analyzed by RT-PCR. The PCR products derived from mRNA and genomic DNA could be distinguished (447 and 552 bp, respectively). Left panel: RNAs were prepared from E, 0-24 h embryos; 1L, first instar larvae; 2L, second instar larvae; 3L, third instar larvae; EP, early pupae; and LP, late pupae. Right panel: RNAs were prepared from the heads and bodies of male and female adults. As a control, a portion of *rp49* RNA was amplified from the same samples. G, genomic DNA; M, DNA markers.

(B) Amo protein detected by Western blotting. Amo was concentrated from cell culture and fly lysates by immunoprecipitation with anti-Amo antibodies. Western blots were probed with anti-Amo antibodies. Left panel: (left two lanes) HEK293 cells transfected with either an empty vector (pcDNA3) or pcDNA3-*amo* (p-*amo*); (right lanes) male and female bodies. Right panel: lysates were obtained from male bodies of the following genotypes: (1) amo^{+} (wild-type), (2) amo^{1}, (3) amo^{1} mutant flies containing a wild-type amo^{+} transgene (amo^{1}; P [amo^{+}]) and (4) $tudor^{1}$ mutant.

(C) *amo* knockout construct. The *amo* genomic region and the w^{+} minigene are represented by the blue and red boxes, respectively. The orientation of the *amo* gene is indicated, and the positions of the stop codons are indicated by the vertical arrows.

(D) Reduced fertility in amo^{1}. Single-pair matings between w^{1118} females and males of the following genotypes were allowed to proceed for 24 hr before the males were removed: (1) w^{1118} (wild-type), (2) amo^{1}, and (3) amo^{1} mutant flies with the amo^{+} transgene (amo^{1};P [amo^{+}]). Females remained in the vials for an additional 48 hr. The number of vials that produced progeny within the indicated ranges is shown.

(E) The average number of progeny was reduced in matings between wild-type females and amo^{1} males. The averages are based on the same data presented in panel (C) (amo^{1}: 0.6 ± 0.2 (SEM). Wild-type, 84 ± 3.4. amo^{1};P [amo^{+}], 88 ± 5.1.

We next investigated possible post-copulatory defects. Wild-type males deposit thousands of sperm, together with accessory gland products, as a compact mass in the anterior uterus. We found that *amo* sperm were successfully transferred to the females. Similar sperm masses and comparable numbers of sperm nuclei were found in females shortly after mating with either wild-type (Figures 3A and 3B) or amo^{1} males (Figures 3C and 3D).

After deposition in the uterus, sperm must move into specialized storage organs that branch from the anterior end of the uterus [17]. The major organ, which holds 65%–80% of stored sperm, is the seminal receptacle, a long coiled tube with a cuticle-lined lumen. A pair of mushroom-shaped spermathecae stores the remaining sperm, probably for longer-term storage. Sperm storage enables sperm to be used for up to several weeks after a single mating. Approximately 20% of sperm are stored and used in fertilization; the remainder are expelled from the uterus within a few hours of mating.

To address whether Amo was required for sperm storage, we dissected seminal receptacles and spermathecae from wild-type females that had been mated to amo^{1} and wild-type males from 30 min to 24 hr after the start of copulation. Wild-type sperm normally begin to enter storage organs during copulation, and the storage organs are typically filled within 2 hr (Figures 3E, 3F, and 3J). However, we detected few or no amo^{1} mutant sperm in seminal receptacles (Figures 3G, 3H, and 3J), indicating that they rarely entered the storage organs. Storage of mutant sperm in spermathecae was also reduced. We found sperm in 36 of 38 spermathecae dissected from females mated to amo^{+} males. In contrast, only 31 of 57 spermathecae from females mated to amo^{1} mutants contained sperm, and most of these spermathecae were not filled. The few progeny that emerged from matings between amo^{1} males and wild-type females were healthy, indicating that the amo^{1} sperm were otherwise functional.

To provide additional evidence that there was a sperm storage defect associated with amo^{1} sperm, we conducted sperm competition assays. Sperm competition occurs when a female mates with more than one male [18] and, in flies, sperm derived from the last male to mate with a female has a significant competitive advantage. Typically, at least 80% of the progeny (>0.8 P2

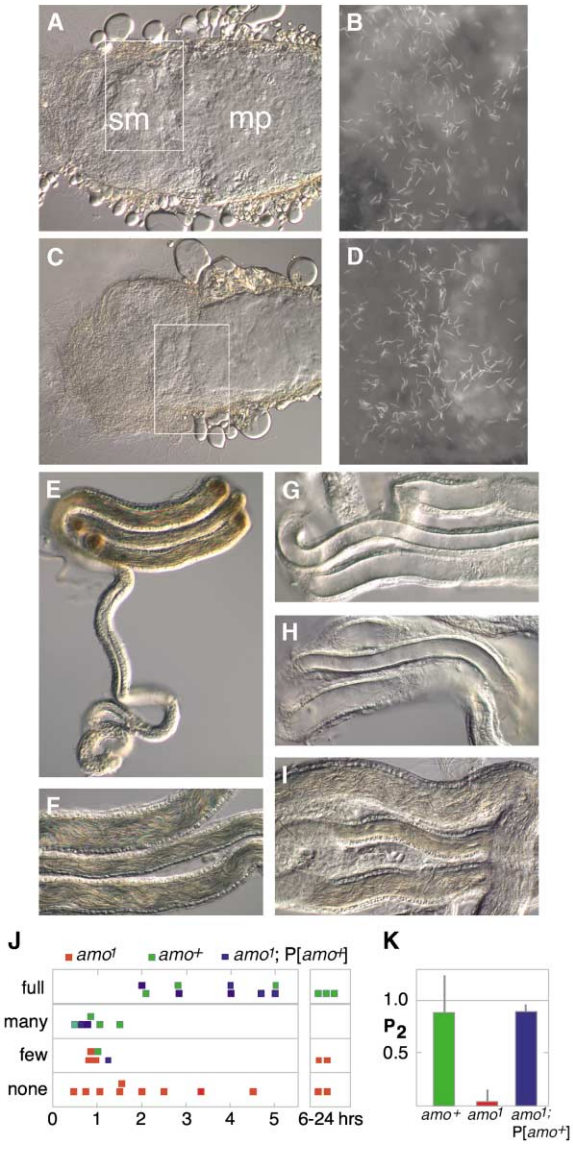

Figure 3. Sperm Storage and Sperm Competition Defects in *amo*^{1} Mutant Sperm

(A–D) Sperm masses (sm) and mating plugs (mp) from uteri of recently mated *w*^{1118} females, stained with DAPI to show sperm nuclei ([B and D]; areas correspond to boxes in [A] and [C], respectively). Sperm masses were dissected from females mated to *amo*$^{+}$ (A and B) and *amo*^{1} (C and D) males 1–1.5 hr after mating.

(E) Partly uncoiled seminal receptacle from a *w*^{1118} female, dissected 1 hr after mating to an *amo*$^{+}$ male and containing sperm in the distal lumen.

(F) Part of the distal receptacle (from [E]) at higher magnification. Many sperm are present, but the receptacle is not yet full. Sperm motility is seen as color fringing from successive exposures.

(G) Distal receptacle dissected 1.5 hr after mating to an *amo*^{1} male. No sperm were present.

(H) Distal receptacle dissected 12 hr after mating to *amo*^{1}. A few sperm were present.

(I) Distal receptacle dissected 2 hr after mating to an *amo*^{1};P[*amo*$^{+}$]/+ male.

(J) Timeline summary of sperm storage in hours. Receptacles dissected at various times after the start of copulation with the indicated males were categorized as containing the following: (i) no sperm (e.g., panel [G]); (ii) fewer than 10 sperm (e.g., [H]); (iii) many sperm but with motility indicating incomplete filling (e.g., [F]); and (iv) sperm completely filling the receptacle with no room for motility (e.g., [I]).

(K) Results of a second-male mating assay, showing reduced competitive ability of *amo*^{1} mutant sperm. *w*^{1118} females were mated first to standard *w*$^{+}$;*amo*$^{+}$ males, then individually remated to *w*^{1118} males of the different *amo* genotypes shown. P2, the proportion of offspring sired by the second males, was calculated as the proportion of *w*^{1118} daughters among all female offspring.

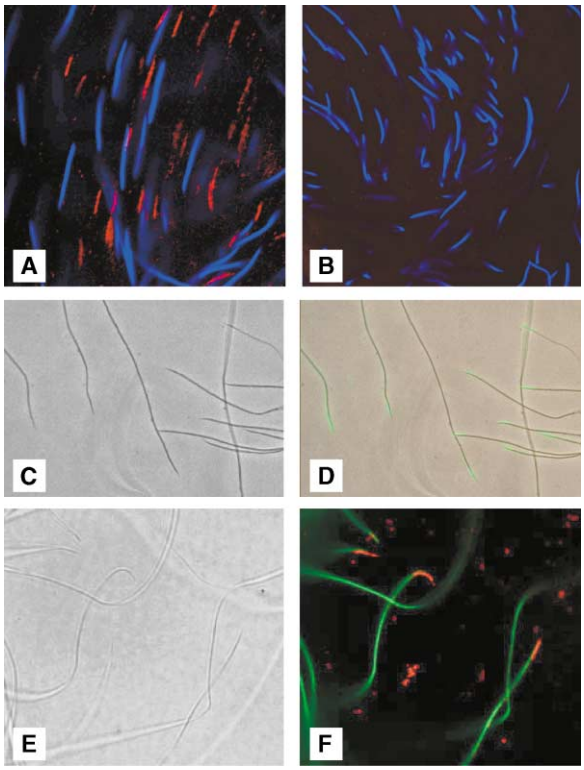

Figure 4. Amo Is Concentrated at the Posterior Tip of the Sperm Flagella

(A and B) Amo staining is absent in *amo*^{1} mutant testes. Seminal vesicles were dissected from (A) wild-type and (B) *amo*^{1} males and stained with TOTO-3 nucleic acid stain and anti-Amo antibodies. The anti-Amo staining was detected with Alexa Fluor 488 goat-anti-rabbit IgG. The anti-Amo and nuclear staining were red and blue, respectively. Only a subset of the sperm tips were labeled with anti-Amo. This region of the dissociated sperm mass is shown because it includes a high proportion of anti-Amo positive ends.

(C and D) Amo is concentrated at the sperm tip. Sperm were dissected from testis, separated from the sperm mass, and stained with anti-Amo. (C) Phase contrast image of wild-type sperm. (D) Same sperm shown in (C) stained with anti-Amo (green). The immunostaining is supeimposed on the phase constrast image.

(E and F) Amo localizes to the posterior tip of the sperm. (E) DIC image of wild-type sperm separated from a sperm mass. (F) Same sperm as in (E) showing the merged images of the Don Juan-GFP marker (green) and anti-Amo staining (red).

value) are derived from sperm introduced by the last male. The ability to enter and remain in storage organs is a major component of sperm competitive ability in multiply mated *Drosophila* [18]. Wild-type (*w; amo*$^{+}$) and *w*; *amo*^{1} males were mated to wild-type (*w*) females, 2 days after they had mated with a standard wild-type (*w*$^{+}$) male. Sperm from wild-type second males showed

the expected high degree of success in the competition assay (Figure 3K). In contrast, *amo[1]* mutant sperm were unable to compete with sperm introduced by the first males (Figure 3K). This finding is consistent with the sperm storage defect described above.

Because our results suggest that Amo plays a functional role in mature sperm, we stained sperm with anti-Amo antibodies. We found that anti-Amo stained wild-type but not *amo[1]* seminal vesicles (Figures 4A and 4B). Moreover, the anti-Amo staining was concentrated at one tip of the sperm (Figures 4C and 4D). It appeared that just one end of the sperm contained Amo because only some of the sperm tips were labeled with anti-Amo (data not shown). The region of the dissociated sperm mass shown (Figures 4C and 4D) is included because it contains a particularly high proportion of anti-Amo positive tips. To determine whether Amo was present at the anterior or posterior tip of the sperm, we compared the distribution of the anti-Amo staining with that of DAPI and a sperm-enriched mitochondrial marker, Don Juan-GFP. This marker labels the sperm's distal region, beginning just posterior to the nucleus and extending nearly to the posterior tip [19]. The placement of the nucleus is highly asymmetric, such that the head region is much shorter than the tail. In no case did we detect anti-Amo staining anterior to the DAPI signal, which was also devoid of the Don Juan-GFP signal (e.g., Figure S2). We found the anti-Amo staining was posterior to the Don Juan-GFP, demonstrating that the labeling was at the posterior tip of the sperm (Figures 4E and 4F; Figure S2).

The preceding data demonstrate that Amo is localized to sperm and is critical for male fertility. Characterization of the *amo[1]* phenotype revealed that mutant sperm were transferred to the uterus and were motile. However, *amo[1]* sperm failed to move into the female storage organs, which formed the basis for the dramatic reduction in fertility. Very little is known concerning the mechanisms that target sperm to the female storage organs. To date, the only other protein known to be required for sperm storage is a secreted glycoprotein, Acp36DE, which is transferred to the female with the seminal fluid [20].

Given the *amo[1]* phenotype, gross sperm motility does not appear to be sufficient for appropriate entry of sperm into the seminal receptacle and spermathecae. Furthermore, the enormous length of the *Drosophila* sperm tail relative to the confined space in the storage organs and reproductive tract suggest that conventional flagellar swimming is unlikely to propel sperm into the storage organs. One intriguing possibility is that Amo transduces a signal that results in subtle stereotypical movements that may be necessary for sperm to enter the small openings of the storage organs. Alternatively, Amo could form part of a complex involved in recognition of cues from the female reproductive tract, and these cues could be necessary for entry into the storage organs. Whether polycystin-2 plays a role in mammalian sperm function remains an open question because mice with null mutations in either *pkd1* or *pkd2* die in utero [21, 22]. In conclusion, the finding that Amo functions in the sperm flagella supports an emerging concept that polycystin-2-related proteins have an important and evolutionarily conserved role in a broad array of ciliary structures.

Supplemental Data

Supplemental Experimental Procedures as well as two additional figures are available with this article online at http://www.current-biology.com/cgi/content/full/13/24/2179/DC1/.

Acknowledgments

We thank Dr. D. Murphy and the Microscopy Facility at the Johns Hopkins University School of Medicine for help with the microscopy and Dr. K. Golic for the fly stocks and vectors for performing the homologous recombination. T.J.W. was supported by National Institutes of Health K08 (DK02562) and Polycystic Kidney Disease Foundation Grant in AID (13A2R), and M.J.K. was supported by a grant from the PKD Foundation (24A2R). This work was supported by the PKD Center of Excellence (National Institutes of Health P50-DK57325) and the National Eye Institute (EY10852).

Received: September 22, 2003
Revised: October 20, 2003
Accepted: October 21, 2003
Published: December 16, 2003

References

1. Sutters, M., and Germino, G.G. (2003). Autosomal dominant polycystic kidney disease: molecular genetics and pathophysiology. J. Lab. Clin. Med. *141*, 91–101.
2. Montell, C. (2001). Physiology, phylogeny and functions of the TRP superfamily of cation channels. *Science's STKE*, http://stke.sciencemag.org/cgi/content/full/OC_sigtrans;2001/90/re1.
3. Qian, F., Germino, F.J., Cai, Y., Zhang, X., Somlo, S., and Germino, G.G. (1997). PKD1 interacts with PKD2 through a probable coiled-coil domain. Nat. Genet. *16*, 179–183.
4. Tsiokas, L., Kim, E., Arnould, T., Sukhatme, V.P., and Walz, G. (1997). Homo- and heterodimeric interactions between the gene products of *PKD1* and *PKD2*. Proc. Natl. Acad. Sci. USA *94*, 6965–6970.
5. Yoder, B.K., Hou, X., and Guay-Woodford, L.M. (2002). The polycystic kidney disease proteins, polycystin-1, polycystin-2, polaris, and cystin, are co-localized in renal cilia. J. Am. Soc. Nephrol. *13*, 2508–2516.
6. Pazour, G.J., San Agustin, J.T., Follit, J.A., Rosenbaum, J.L., and Witman, G.B. (2002). Polycystin-2 localizes to kidney cilia and the ciliary level is elevated in orpk mice with polycystic kidney disease. Curr. Biol. *12*, R378–R380.
7. Barr, M.M., DeModena, J., Braun, D., Nguyen, C.Q., Hall, D.H., and Sternberg, P.W. (2001). The *Caenorhabditis elegans* autosomal dominant polycystic kidney disease gene homologs *lov-1* and *pkd-2* act in the same pathway. Curr. Biol. *11*, 1341–1346.
8. McGrath, J., Somlo, S., Makova, S., Tian, X., and Brueckner, M. (2003). Two populations of node monocilia initiate left-right asymmetry in the mouse. Cell *114*, 61–73.
9. Mochizuki, T., Wu, G., Hayashi, T., Xenophontos, S.L., Veldhuisen, B., Saris, J.J., Reynolds, D.M., Cai, Y., Gabow, P.A., Pierides, A., et al. (1996). *PKD2*, a gene for polycystic kidney disease that encodes an integral membrane protein. Science *272*, 1339–1342.
10. Nomura, H., Turco, A.E., Pei, Y., Kalaydjieva, L., Schiavello, T., Weremowicz, S., Ji, W., Morton, C.C., Meisler, M., Reeders, S.T., et al. (1998). Identification of *PKDL*, a novel polycystic kidney disease 2-like gene whose murine homologue is deleted in mice with kidney and retinal defects. J. Biol. Chem. *273*, 25967–25973.
11. Wu, G., Hayashi, T., Park, J.H., Dixit, M., Reynolds, D.M., Li, L., Maeda, Y., Cai, Y., Coca-Prados, M., and Somlo, S. (1998). Identification of *PKD2L*, a human *PKD2*-related gene: tissue-specific expression and mapping to chromosome 10q25. Genomics *54*, 564–568.
12. Guo, L., Schreiber, T.H., Weremowicz, S., Morton, C.C., Lee, C., and Zhou, J. (2000). Identification and characterization of a novel

polycystin family member, polycystin-L2, in mouse and human: sequence, expression, alternative splicing, and chromosomal localization. Genomics *64*, 241–251.
13. Mahowald, A.P. (2001). Assembly of the Drosophila germ plasm. Int. Rev. Cytol. *203*, 187–213.
14. Rong, Y.S., and Golic, K.G. (2000). Gene targeting by homologous recombination in Drosophila. Science *288*, 2013–2018.
15. Rong, Y.S., and Golic, K.G. (2001). A targeted gene knockout in Drosophila. Genetics *157*, 1307–1312.
16. Rong, Y.S., Titen, S.W., Xie, H.B., Golic, M.M., Bastiani, M., Bandyopadhyay, P., Olivera, B.M., Brodsky, M., Rubin, G.M., and Golic, K.G. (2002). Targeted mutagenesis by homologous recombination in *D. melanogaster*. Genes Dev. *16*, 1568–1581.
17. Bloch Qazi, M.C., Heifetz, Y., and Wolfner, M.F. (2003). The developments between gametogenesis and fertilization: ovulation and female sperm storage in *Drosophila melanogaster*. Dev. Biol. *256*, 195–211.
18. Gromko, M., Gilbert, D., and Richmond, R. (1984). Sperm transfer and use in the multiple mating system of Drosophila. In Sperm Competition and the Evolution of Animal Mating Systems, R.L. Smith., ed. (Orlando, FL: Academic Press), pp. 371-426.
19. Santel, A., Blümer, N., Kämpfer, M., and Renkawitz-Pohl, R. (1998). Flagellar mitochondrial association of the male-specific Don Juan protein in *Drosophila* spermatozoa. J. Cell Sci. *111*, 3299–3309.
20. Neubaum, D.M., and Wolfner, M.F. (1999). Mated *Drosophila melanogaster* females require a seminal fluid protein, Acp36DE, to store sperm efficiently. Genetics *153*, 845–857.
21. Wu, G., D'Agati, V., Cai, Y., Markowitz, G., Park, J.H., Reynolds, D.M., Maeda, Y., Le, T.C., Hou, H., Jr., Kucherlapati, R., et al. (1998). Somatic inactivation of *Pkd2* results in polycystic kidney disease. Cell *93*, 177–188.
22. Lu, W., Peissel, B., Babakhanlou, H., Pavlova, A., Geng, L., Fan, X., Larson, C., Brent, G., and Zhou, J. (1997). Perinatal lethality with kidney and pancreas defects in mice with a targetted *Pkd1* mutation. Nat. Genet. *17*, 179–181.

Accession Number

The Genbank accession number for the *amo* cDNA sequence is AY437926.